TASK QUARTERLY 10 No 3, 227–238

NUMERICAL SIMULATIONS OF IMPULSIVELY EXCITED FAST MAGNETOSONIC WAVES IN TWO PARALLEL SLABS

RAFAŁ OGRODOWCZYK[1] AND KRZYSZTOF MURAWSKI[2]

[1] *Institute of Mathematics and Computer Sciences, The State University in Chełm, Pocztowa 54, 22-100 Chełm, Poland*
rogrodow@pwsz.chelm.pl

[2] *Institute of Physics, UMCS, Radziszewskiego 10, 20-031 Lublin, Poland*

(Received 10 February 2006; revised manuscript received 21 April 2006)

Abstract: We present numerical results of a temporal evolution of impulsively excited magnetosonic waves in a solar coronal loop that is approximated by a set of two straight plasma slabs of mass density enhancement. Numerical simulations reveal that shapes of wavelet spectra of time signatures of these waves depend on a distance between the strands and on a position of the initial pulse. We find that with a distance growing between these strands short period waves contribute more while long period waves contribute less to the wavelet spectra. We demonstrate that a presence of the second parallel strand affects considerably wave propagation in comparison to one strand alone. We find out that the initial pulse triggers a packet of propagating waves among witch sausage and kink modes are present simultaneously.

Keywords: Sun: MHD, Sun: corona, Sun: oscillation

1. Introduction

It has long been established both on theoretical and observational grounds that magnetohydrodynamic (MHD) waves can be sustained by solar coronal loops (*e.g.* [1, 2]). The recent interest in wave propagation in solar coronal loops (see *e.g.* [3–5]), spurred on by SOHO and TRACE observations [6–8], has highlighted the complexity in a development of realistic models (*e.g.* [9]). The usual approach is to treat a coronal loop as a homogeneous magnetic column of a condensed plasma [5]. Such an approach leads to dispersion relations which describe the normal modes of the system [10–12] and numerical solutions of the full set of magnetohydrodynamic (MHD) equations (*e.g.* [13]).

Solar coronal loops support both propagating and standing MHD waves. Propagating slow magnetosonic waves were detected near the footpoints of coronal loops

[14, 15]. Standing slow waves were discussed by [9, 16–18]. Propagating fast magnetosonic waves in monolithic coronal loops were studied recently by *e.g.* [6, 17, 19]. Among the standing waves observed in coronal loops are the transverse [20], vertical [21] global kinks and sausage mode oscillations [22].

Studies of a structured coronal loop are rare. We distinguish the work done by [5]. It was proved by numerical simulations that a presence of two parallel slabs affects considerably wave propagation [23]. It was suggested by [24] that a coronal loop consists of multi-threads or fibrils. An interaction between oscillating fibrils in such system was studied by [5], who showed that waves frequencies of fast magnetosonic modes is the same in identical fibrils. The most recent analysis of the observational TRACE data leads to a conclusion that a structure of a coronal loop is complex, consisting of a multiple of strands [7, 8]. It was found that elementary loops are near-isothermal with their width of 2 Mm as well as wider loops have heterogeneous structure and a single loop is build from 10 strands even. While wave analysis in such complex structures seems to be difficult numerical simulations are enough amenable to lead to reliable results.

A main purpose of this paper is to establish *an influence of the strands stratification of a coronal loop* on propagating waves trains. We adopt a slab as a simple model of a loop strand and perform parametric studies which allow us to determine an influence of a second strand on wave propagation in a loop that consists of two strands.

This paper is organized as follows. Sections 2 and 3 describe physical and numerical models, respectively. Results of numerical simulations are presented in Section 4. This paper is concluded by a summary of the main results in Section 5.

2. Physical model

Consider an ideal, perfectly conducting, compressible plasma. Such a plasma can be described by the time-dependent ideal MHD equations:

$$\frac{\partial \varrho}{\partial t} + \nabla \cdot (\varrho \mathbf{V}) = 0, \tag{1}$$

$$\varrho \frac{\partial \mathbf{V}}{\partial t} + \varrho (\mathbf{V} \cdot \nabla) \mathbf{V} = -\nabla p + \frac{1}{\mu} (\nabla \times \mathbf{B}) \times \mathbf{B}, \tag{2}$$

$$\frac{\partial p}{\partial t} + \nabla \cdot (p \mathbf{V}) = (1-\gamma) p \nabla \cdot \mathbf{V}, \tag{3}$$

$$\frac{\partial \mathbf{B}}{\partial t} = \nabla \times (\mathbf{V} \times \mathbf{B}), \tag{4}$$

$$\nabla \cdot \mathbf{B} = 0. \tag{5}$$

Here ϱ is mass density, $\mathbf{V}$ is flow velocity, $\mathbf{B}$ is magnetic field, p is gas pressure, μ is the magnetic permeability, and $\gamma = 5/3$ is the adiabatic index.

Henceforth, we limit our discussion to a two-dimensional atmosphere for which the plasma quantities are independent of the spatial coordinate y, *i.e.* $\partial/\partial y = 0$, and $\mathbf{V}_{\rm y} = \mathbf{B}_{\rm y} = 0$. While a recently observed loop was showed to be collected of 10 strands [8], we consider a simple model in which a loop consists of two parallel identical strands which are separated by a distance d (Figure 1). A half-width of such strand is denoted by w. We assume that all plasma quantities experience a sudden jump

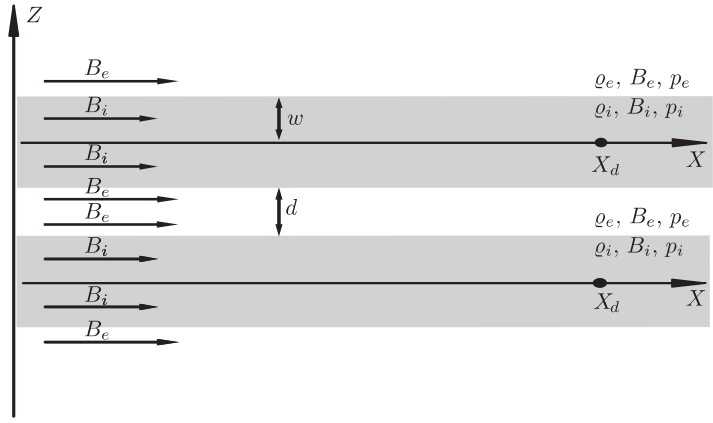

Figure 1. A geometry of the model. The symbol X_d denotes a position of a detector and d is a distance between the strands. Shaded regions correspond to the plasma slabs of enhanced mass density, with their half-width w

from their constant values in the ambient medium to their constant values inside each strand. The ambient values are denoted by the subscript e, while the internal quantities possess the subscript i (Figure 1).

We define a sound speed, c_se, and the Alfvén speed, V_Ae, in the ambient medium, as $c_\mathrm{se}^2 = \gamma p_\mathrm{e}/\varrho_\mathrm{e}$ and $V_\mathrm{Ae}^2 = B_\mathrm{e}/\mu\varrho_\mathrm{e}$. The plasma β in the ambient medium is expressed by the ratio of Alfvén speeds, $v = V_\mathrm{Ae}/V_\mathrm{Ai}$, temperature ratio $T_\mathrm{i}/T_\mathrm{e}$, and mass density ratio $r = \varrho_\mathrm{i}/\varrho_\mathrm{e}$. It is given as:

$$\beta = \frac{p_\mathrm{e}}{B_\mathrm{e}^2/(2\mu)} = \frac{1}{\frac{T_\mathrm{i}}{T_\mathrm{e}} r - 1} \frac{v^2 - r}{v^2}. \tag{6}$$

Plasma quantities inside the strands are then:

$$\varrho_\mathrm{i} = r\,\varrho_\mathrm{e}, \quad B_\mathrm{i} = B_\mathrm{e}\frac{\sqrt{r}}{v}, \quad p_\mathrm{i} = p_\mathrm{t} - \frac{B_\mathrm{i}^2}{2\mu}\,. \tag{7}$$

Here the total pressure p_t is defined as the sum of the gas and magnetic pressures, *viz.*:

$$p_\mathrm{t} = p_\mathrm{e} + \frac{B_\mathrm{e}^2}{2\mu}. \tag{8}$$

Values for these parameters are presented in Table 1.

Table 1. Equilibrium parameters

Quantity	Value
V_Ae	$1.0\,\mathrm{Mm\,s^{-1}}$
β	$0.52\cdot 10^{-3}$
ϱ_e	$10^{-15}\,\mathrm{kg\,m^{-3}}$
$T_\mathrm{i}/T_\mathrm{e}$	2
r	10
v	$\sqrt{10.1}$
l	1 Mm
w	2 Mm

Equations (1)–(5) can be linearized and then applied to a single slab to derive a dispersion relation [11]. This dispersion relation describes two sets of modes, namely slow and fast magnetosonic waves. Slow magnetosonic waves propagate with their phase speeds which are close to the sound speed. These waves are weakly dispersive. On the other hand, the fast magnetosonic modes have their phase-speeds in the range $V_{\rm Ai} < \omega/k < V_{\rm Ae}$ and they are strongly dispersive in the long wavelength limit. These wave are divided into *sausage waves* which are symmetric pulsations of the loop, with the central axis of the loop remaining undisturbed and *kink waves* which involve lateral displacement of the loop, maintaining its cross-section, with the axis of the loop resembling a wriggling snake. For a cold plasma (sound speeds $c_{\rm se} = c_{\rm si} = 0$) case the dispersion relation has the form [11]:

$$\tan(nw) = m/n \tag{9}$$

for kink modes and:

$$\tan(nw) = -n/m \tag{10}$$

for sausage modes. Here we set:

$$m^2 = k^2 - \frac{w^2}{V_{\rm Ae}^2}, \qquad n^2 = \frac{w^2}{V_{\rm Ai}^2} - k^2, \tag{11}$$

with k being a wavenumber along the x-direction. It is noteworthy that $m > 0$ corresponds to non-leaky or ducted waves.

To a lack of our knowledge a dispersion relation for the two parallel slabs structure is unknown. A difficulty in a derivation of such dispersion relation results from a cross-talk between these slabs. However, when these slabs become well separated we expect that the cross-talk can be neglected and each slab oscillates independently one from another.

3. Numerical model

We adopt the numerical code EMILY which was developed by [25]. This code is dedicated to solve the time-dependent, non-ideal magnetohydrodynamic equations. Here, it is implemented an algorithm of finite-volume scheme that uses an approximate Riemann solver for the hyperbolic fluxes and central differencing applied on nested control volumes for the parabolic fluxes. The numerical scheme, which was applied in this code, is second-order accurate in space and time.

Equations (1)–(5) are solved numerically with a use of a homogeneous grid of 600×500 numerical cells. This grid covers an Eulerian box $(-30l, 170l) \times (-30l, 30l)$, where l is a spatial unit which is chosen equal to 1Mm. As our purpose is to study propagating waves we used zero-gradient conditions at the boundaries of the simulation region to represent natural extension of the real medium.

We consider initially launched pulses in pressure, *viz.*:

$$p(x,z,t=0) = p_0 \left[1 + A_{\rm p} e^{-x^2/w_{\rm p}^2} e^{-(z-z_0)^2/w_{\rm p}^2}\right], \tag{12}$$

where p_0 is a background pressure ($p_{\rm e}$ or $p_{\rm i}$), $A_{\rm p}$ denotes a relative amplitude of the pulse, z_0 is its initial position along the vertical direction, and $w_{\rm p} = 2w$ its width.

4. Numerical results

In this part of the paper we present results of the parametric studies we have performed. We focus our attention on two parameters: (a) a distance between the strands, d, (b) a pulse position in the z-direction, z_0. We set and hold fixed $x_0 = 0$. We perform wavelet and Fourier analysis which allows to determine an influence of a presence of the second strand on wave spectra in the other strand.

4.1. Sausage waves

We launch the initial pulse inside the lower strand at $z_0 = 0$. Figure 2 displays spatial profiles of mass density ϱ in the two parallel slabs. As these profiles exhibit compressed plasma regions that are followed by rarefied plasma we conclude that the initial pulse excites essentially sausage waves in the bottom strand. As a result of energy leakage from this strand, waves are excited in the top slab. However, it is peculiar that these excited waves are sausage modes but not kink modes. We would expect that a perturbation localized outside the top strand triggers kink modes. This is not a case here. This scenario is determined by a cross-talk between the bottom and top strands. As a consequence of this cross-talk sausage modes result in both strands. Obviously an interaction between sausage modes in the bottom and top strands is stronger than an interaction between sausage and kink modes. As an additional evidence of the cross-talk serves a fact that at $t = 384$s waves in the top slab posses larger amplitudes than oscillations in the bottom slab. This result is a general agreement with the findings made by [26] and [27].

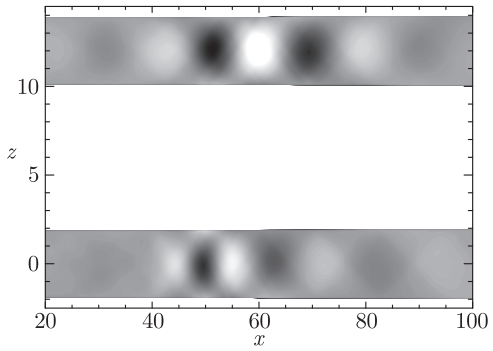

Figure 2. Spatial profiles of mass density, ϱ, resulting from the initial pulse of Equation (12) with $A_p = 2$, $z_0 = 0$ at $t = 384$s. A distance between the strands is $d = 4w$

The cross-talk is evident in time-signatures of wave signals collected on the strands axis (Figure 3). It is evident form Figure 3 that time-signatures collected in the top and bottom strands are essentially similar. While wave amplitudes are of a comparable magnitude, a phase-shift between maxima is discernible. While for the top strand a maximum occurs at $t \simeq 370$s and $t \simeq 430$s, the bottom strand experiences a highest compression at $t \simeq 400$s. This phase-shift can be traced in wavelet spectra of the time-signatures (Figure 4). It is interesting that these spectrum consist of three wave-periods which appear in the wavelet and FFT spectrum. One of them is dominant ($P \simeq 22$s) and the rest of them have periods $P \simeq 61$s and $P \simeq 69$s. Indeed, we can

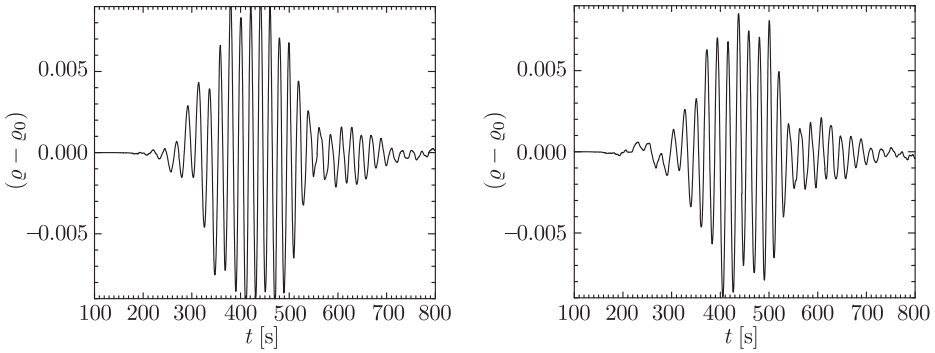

Figure 3. Time-signatures of the wave signals, collected at $x_\mathrm{d} = 140l$ inside the upper (left panel) and lower (right panel) strands in the case of Figure 2

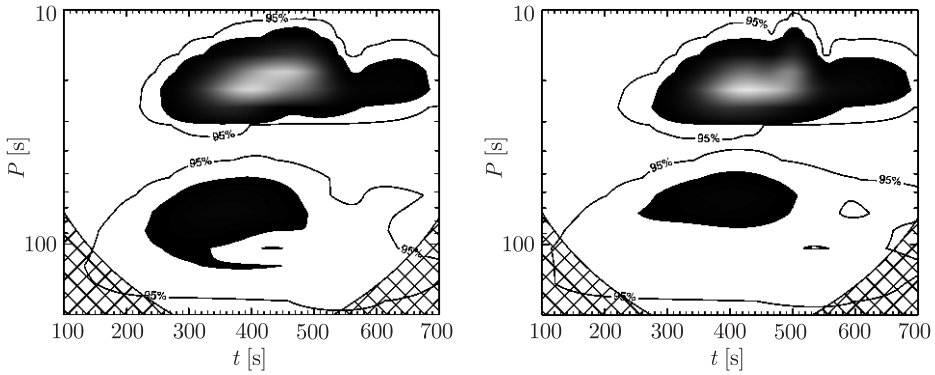

Figure 4. Wavelet spectra of the wave signals of Figure 3

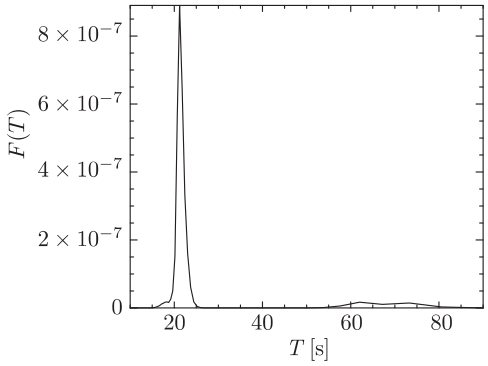

Figure 5. Fourier spectra of the wave signal of Figure 3

estimate the precise values of dominant wave periods from the left panel of Figure 4 and Figure 5.

4.2. Kink waves

The initial pulse was launched outside the slab at: (a) $z_0 = -5l$ and (b) $z_0 = 6l$. Figure 6 shows the corresponding spatial profiles of mass density ϱ. We would expect that the initial pulse launched outside a strand triggers kink modes only. However,

in this case we find that the initial pulse excites kink and sausage modes in both strands. This scenario is determined by a cross-talk between the bottom and top strands. As a consequence of this cross-talk trapped sausage modes result in both strands although the kink modes remain dominant there. In the case of the initial pulse launched between the strands, Fourier amplitudes associated with the kink and sausage modes are comparable (Figure 7). We conclude that a presence of the second strand results in an excitation of sausage modes in the system.

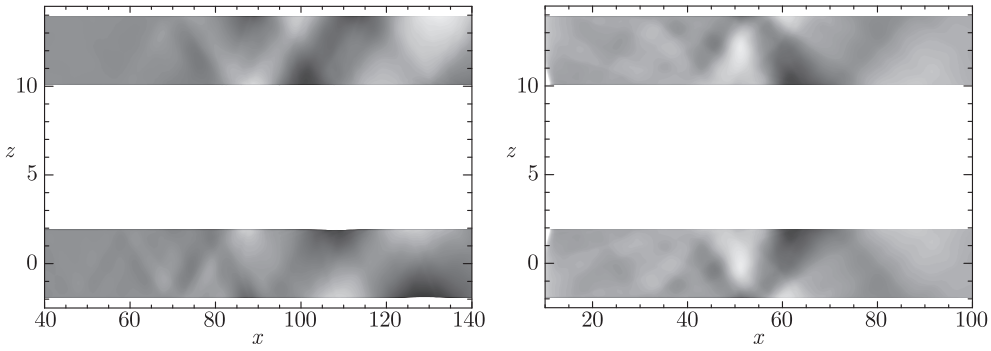

Figure 6. Spatial profiles of the mass density, ϱ, resulting from the initial pulse of Equation (12) with $A_{\mathrm{p}} = 2$, $z_0 = -5l$ at $t = 288$s (left panel), and $z_0 = 6l$ at $t = 384$s (right panel). A distance between the slabs is $d = 4w$

4.3. Modes identification

In this part of the paper we direct our efforts towards identification of modes which are excited in the system. We adopt the dispersion relations for a magnetic slab alone [11] (see Equations (10)–(11)).

Figure 8 displays wave frequency ω versus horizontal wavenumber k, which follow from the dispersion relations of Equations (10)–(11). Solid and dotted lines correspond to respectively kink and sausage oscillations. It is noteworthy that the first-order ($n = 1$) kink mode that is represented by the lowest solid line is a ducted wave for all values of k. The remnant modes exist as trapped waves for sufficiently large values of k. Long waves are called leaky as they propagate in the ambient medium and they transfer energy from a slab to its neighborhood. The initial pulse launched at $z_0 = 0$ excites the second-order ($n = 2$) sausage modes in the slab (left panel of Figure 8). Moving this pulse to $z_0 = -5l$, $n = 1$ and $n = 3$ kink modes are triggered.

Figure 9 illustrates dispersive curves for fast magnetosonic waves propagating along a single slab, in a limit of a cold plasma approximation. Vertical and horizontal lines correspond to wave numbers and wave frequencies, obtained by FFT analysis *of spatial resolution and time-signatures of wave signal of fast magnetosonic waves propagating* in the bottom strand. This strand is settled at the distance $d = 4w$ form the top strand. The top-left (top-right) panel of Figure 9 should be compared with the left (right) panel of Figure 8. It is noteworthy that the second-order sausage mode is present both in the single strand alone (left panel of Figure 8) and in the system of two strands (top-left panel of Figure 9). As a result of a presence of the top

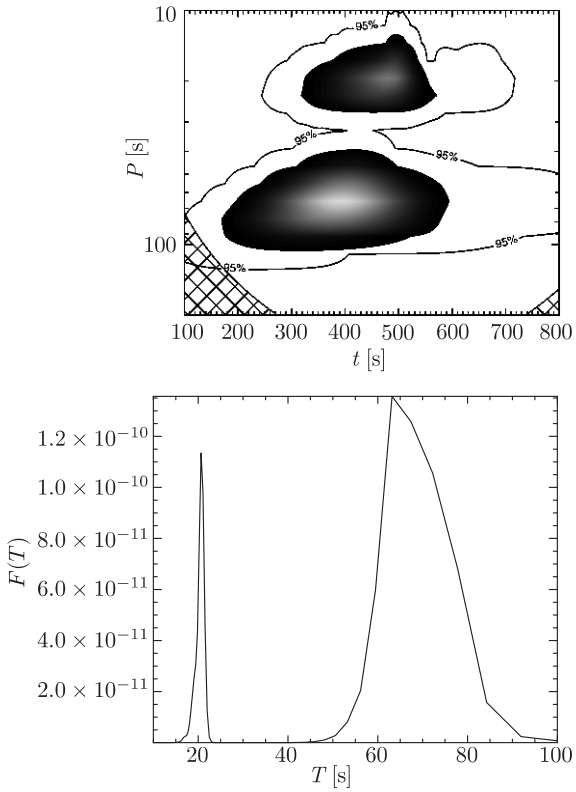

Figure 7. Wavelet (top panel) and Fourier (bottom panel) spectra of the wave signals; the case of Figure 6

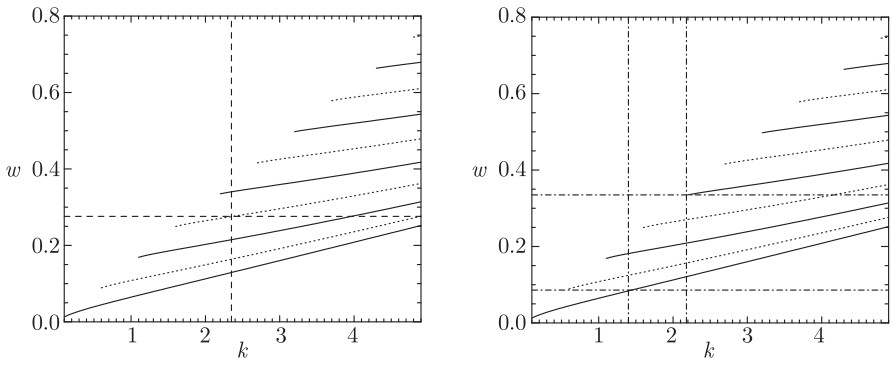

Figure 8. Dispersive curves for fast magnetosonic waves in a case of the top strand is removed from the system: solid (dotted) lines represent kink (sausage) modes, dashed and dashed-dotted lines correspond to a case of the initial pulse launched at $z_0 = 0$ (left panel) and $z_0 = -5l$ (right panel)

strand two additional modes are triggered in the bottom strand. They are identified as $n = 1$ sausage and $n = 1$ kink modes. In a case of the initial pulse is launched below the bottom slab, at $z_0 = -5l$ (top-right panel of Figure 9) $n = 1$ and $n = 2$ sausage additional modes are excited in comparison to a single slab alone (Figure 8). A presence of these modes serves as an evidence of a cross-talk between the strands.

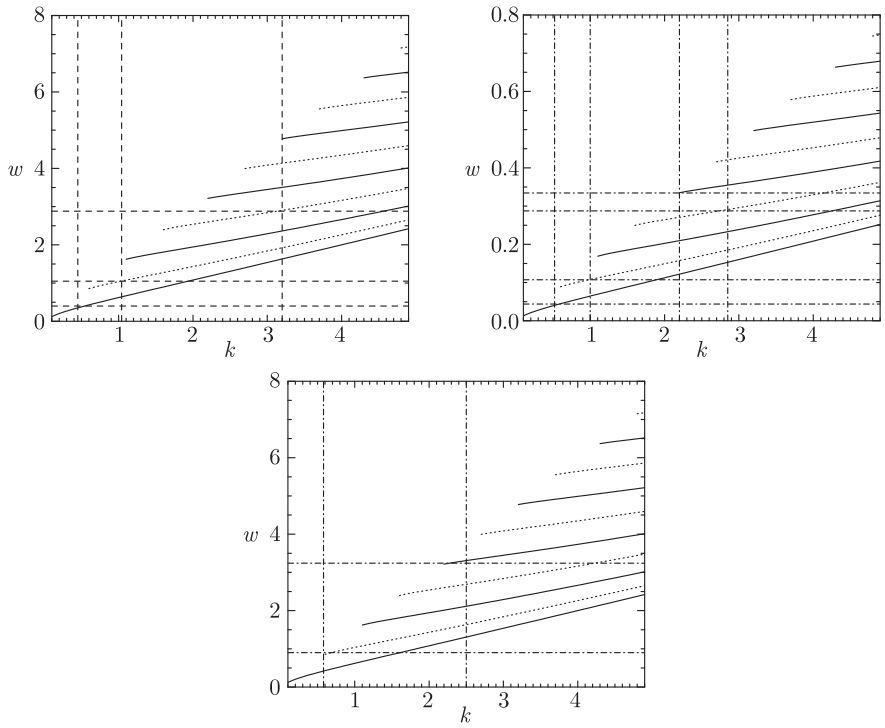

Figure 9. Dispersive curves for fast magnetosonic waves: solid lines represent kink modes and dotted lines correspond to sausage modes for a single strand, dashed and dashed-dotted lines correspond to wave spectra evaluated for a case of two strands, the initial pulse launched at $z_0 = 0$ (top-left panel), $z_0 = -5l$ (top-right panel) and $z_0 = 6l$ (bottom panel); a distance between the strands is $d = 4w = 8l$

When the initial pulse is launched in the region between two strands, at $z_0 = 6l$, $n = 1$ sausage and $n = 3$ kink modes are excited. Although a presence of the kink mode is not surprising, the sausage mode seems to be a result of the cross-talk.

4.4. Parametric studies

Figure 10 illustrates wavelet spectra for two values of a normalized distance between the strands, $d' = d/w$, namely, $d' = 2$ (left panel) and $d' = 8$ (right panel). The initial pulse is launched at $z_0 = 0$ in a system of two strands. It is clearly visible that for the case of d' the wavelet spectrum is reminiscent of the one slab case (not shown). It is discernible that larger wave periods P start to be present in wavelet spectra for low values of d'. We conclude that for a small distance between the strands the effective half-width of the loop is increased and longer wavelength wave packets, comparable to this half-width, are strongly trapped by such system.

Figure 11 illustrates the wave frequency ω versus normalized distance $d' = d/w$ between strands. The triangles and squares correspond to kink and sausage modes, respectively. The number near the symbol denotes the order of a mode. The top-left panel shows ω for the initial pulse launched at $z_0 = 0$. It is discernible that ω is smaller for larger values of d'. We conclude that kink modes result from a presence of second strand in the system.

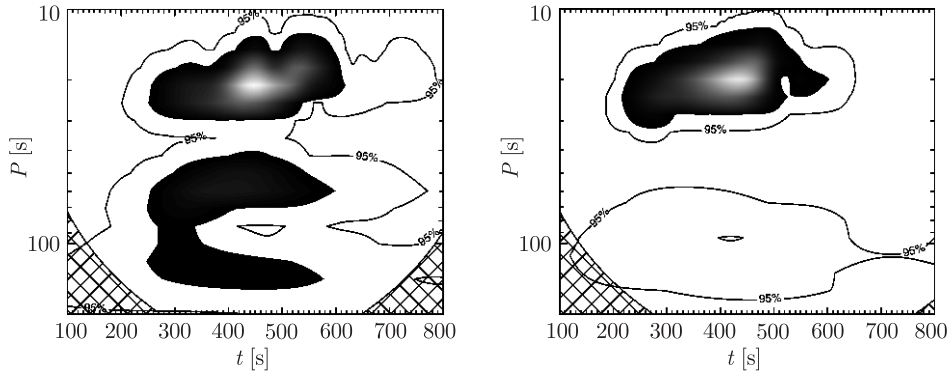

Figure 10. Wavelet spectra of wave signals, collected on the strand axis at $x_{\rm d} = 140l$, $z_{\rm d} = 0$, for the initial pulse launched at $z_0 = 0$; a distance between the strands is: $d' = 2$ (left panel) and $d' = 8$ (right panel)

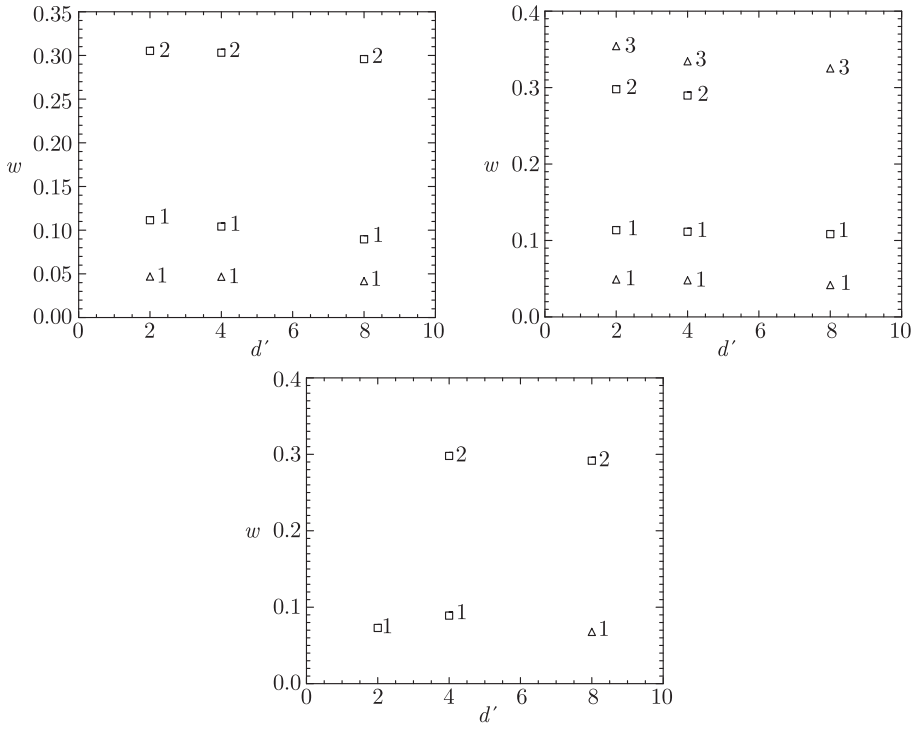

Figure 11. Wave frequency ω vs normalized distance $d' = d/w$ between strands: initial pulse launched at $z_0 = 0$ (top-left panel), $z_0 = -5l$ (top-right panel) and $z_0 = d'/2$ (bottom panel); the triangles (squares) correspond to kink (sausage) modes, the number near the symbol denotes the order of the mode

The top-right panel displays ω for the initial position of the pulse at $z_0 = -5l$. It is noteworthy that the initial pulse launched below the strand's system excites essentially sausage and kink modes. We conclude that this scenario is affected by a cross-talk between the strands. It is noteworthy that only one sausage mode is excited for $d' = 8$, $w = 16l$. For smaller value of d' two sausage modes are presented.

The bottom panel of Figure 11 exemplifies the initial pulse launched at $z_0 = d'/2$ case.

5. Summary

In this paper we performed numerical simulations of impulsively generated magnetosonic waves in a coronal loop which consists of two parallel strands. The results of these simulations reveal that kink and sausage waves possess properties which depend of a distance between the strands. We find that a cross-talk between the strands influences excitation of sausage modes when the initial pulse is launched outside the strands. As a result of this cross-talk, amplitudes of oscillations vary interchangeably in both strands. We identify the modes excited in such system. In comparison to one slab's case additional kink and sausage modes are triggered in the bottom strands. The parametric studies we performed reveal that a wave frequency ω is smaller for larger values of a distance between the strands, d', and a cross-talk phenomenon decreases his influence of the system. It is noteworthy that a smaller number of sausage modes are excited for larger values of d'. On the other hand, it is discernible that larger wave periods P are present in wavelet spectra for smaller d'. We conclude that for a small distance between the strands the effective half-width is increased and wave packets with longer wave period are ducted along the structure.

We conclude that the oscillations of coronal loops observed by TRACE (*e.g.* [21]) could be excited by propagating fast magnetosonic pulse that results from a flare. The period of the observed oscillations is determined by the geometry of the loops, as well as by the magnetic and the density structure of the loops. We find that the period of these oscillations is different in a case such loop is not monolithic but instead it consists of two parallel slabs.

Acknowledgements

KM's work was financially supported by a grant from the State Committee for Scientific Research Republic of Poland, with KBN grant No. 2PO3D 016 25. The magnetohydrodynamics code used in this study was developed at the University of Washington by Ogden S. Jones, Uri Shumlak, Scott Eberhardt, Bogdan Udrea, and provided through the sponsorship of AFOSR program. Wavelet software was written by C. Torrence and G. Compo, and is available at URL: http://paos.colorado.edu/research/wavelets.

References

[1] Roberts B, Edwin P M and Benz A O 1984 *ApJ* **279** 857
[2] Aschwanden M J 1987 *Sol. Phys.* **111** 113
[3] Nakariakov V M, Tisklauri D, Kelly A, Arber T D and Aschwanden M J 2004 *A&A* **414** L25
[4] Cooper F C, Nakariakov V M and Williams D R 2003 *A&A* **409** 325
[5] Diaz A J, Oliver R, Ballester J L and Roberts B 2004 *A&A* **424** 1055
[6] Nakariakov V M and Ofman L 2001 *A&A* **372** L53
[7] Aschwanden M J and Nightingale R W 2005 *ApJ* **633** 499
[8] Aschwanden M J 2005 *ApJ* **634** 193
[9] Selwa M, Murawski K and Solanki S K 2005 *A&A* **437** 701
[10] Edwin P M and Roberts B 1982 *Sol. Phys.* **76** 239
[11] Edwin P M 1991 *Ann. Geophys.* **9** 188
[12] Leble S 1990 *Nonlinear Waves in Waveguides*, Springer-Verlag

[13] Selwa M and Murawski K 2004 *A&A* **425** 719
[14] Berghmans D and Clette F 1999 *Sol. Phys.* **186** 207
[15] De Moortel I, Ireland J and Walsh R W 2000 *A&A* **355** L23
[16] Taroyan Y, Erdelyi R, Dayle J G and Bradshow S J 2005 *A&A* **438** 713
[17] Nakariakov V M, Arber T D, Ault C E, Katsiyannis A C, Williams D R and Keenan F P 2004 *MNRAS* **349** 705
[18] Ofman L and Wang T 2002 *ApJ* **580** L85
[19] Ogrodowczyk R and Murawski K 2006 *Sol. Phys.* **236** 273
[20] Aschwanden M J, Fletcher L, Schrijver C J and Alexander D 1999 *ApJ* **520** 880
[21] Wang T J and Solanki S K 2004 *A&A* **421** L33
[22] Nakariakov V M, Melnikov V F and Reznikova V E 2003 *A&A* **412** L8
[23] Murawski K 1993 *Acta Astron.* **43** 161
[24] Nightingale R W, Aschwanden M J, Alexander D, Reale F and Peres G 2000 *AAS* **32** 812
[25] Jones O S, Shumlak U and Eberhardt D S 1997 *J. Comput. Phys.* **130** 231
[26] Murawski K 2003 *Turbulence, Waves, and Instabilities in the Solar Plasma*, (Forgcs-Dajka E, Petrovay K and Erdlyi R, Eds.), PADEU **13** 61
[27] Murawski K and Roberts B 1994 *Sol. Phys.* **151** 305